J Inorg Organomet Polym (2010) 20:320–325
DOI 10.1007/s10904-010-9342-0

Synthesis, Characterization, Crystal Structures and Thermal and Fluorescence Studies of Dinuclear and Polymeric Silver(I) Complexes of 5,5-Diethylbarbiturate with 2,5-Dimethylpyrazine and Piperazine Involving Ag–Ag Interactions

Eda Soyer · Fatih Yilmaz · Veysel T. Yilmaz · Orhan Buyukgungor · William T. A. Harrison

Received: 6 January 2010 / Accepted: 3 March 2010 / Published online: 17 March 2010

Abstract Two silver(I) complexes, $[Ag(dmpyz)_2][Ag(barb)_2]$ (**1**) and $\{[Ag(ppz)][Ag(barb)_2]\cdot H_2O\}_n$ (**2**) (barb = 5,5-diethylbarbiturate, dmpyz = 2,5-dimethylpyrazine and ppz = piperazine), have been synthesized and characterized by elemental analyses, IR, thermal analysis (TG-DTA) and single-crystal X-ray diffraction. Complex **1** consists of $[Ag(dmpyz)_2]^+$ and $[Ag(barb)_2]^-$ ions in which the silver(I) ions are linearly coordinated by two dmpyz or two barb ligands. These two ions are connected by strong Ag–Ag interactions (Ag–Ag = 2.896 (1) Å). Complex **2** is a 1D coordination polymer in which the silver(I) ions are bridged by the ppz ligands in a linear fashion, leading to a zigzag chain of $[Ag(ppz)]_n^+$, which interacts with the $[Ag(barb)_2]^-$ units by Ag–Ag interactions of 3.183 (1) Å. The 1D chains are further assembled to form 3D networks by strong N–H···O and OW–H···O hydrogen bonds. IR spectra and TG-DTA data are in agreement with the crystal structures. The fluorescent properties of **1** were also evaluated.

E. Soyer · V. T. Yilmaz (✉)
Department of Chemistry, Faculty of Arts and Sciences, Uludag University, 16059 Bursa, Turkey
e-mail: vtyilmaz@uludag.edu.tr

F. Yilmaz
Department of Chemistry, Faculty of Arts and Sciences, Rize University, 53100 Rize, Turkey

O. Buyukgungor
Department of Physics, Faculty of Arts and Sciences, Ondokuz Mayis University, 55139 Kurupelit, Samsun, Turkey

W. T. A. Harrison
Department of Chemistry, University of Aberdeen, Meston Walk, Aberdeen AB24 3UE, Scotland, UK

Keywords 5,5-Diethylbarbiturate · 2,5-Dimethylpyrazine · Piperazine · Coordination polymer · Ag–Ag interactions

1 Introduction

Barbituric acid (also named malonylurea or 6-hydroxyuracil) is not pharmacologically active. Its derivatives usually act as nervous system depressants producing sedation and hypnotic effects. Studies show that the drug action depends on chemical structure and increases with disubstitution of the C5 atom of the pyrimidine ring by ethyl or larger nonpolar groups [1, 2].

Barbituric acids are weak acids that readily deprotonate in solutions to form the corresponding barbiturate anions. The first metal complex of 5,5-diethylbarbiturate (barb) with pyridine (py) was isolated by Zwicker [3] and formulated as $[Cu(barb)_2(py)_2]$. The clinically important barbiturates and their metal complexes were identified by IR spectroscopy [4–6] and the coordination mode of these drugs was suggested on the basis of IR data. However, X-ray crystal structures of metal barbiturate complexes show that barbiturates are polyfunctional ligands with several potential donor sites such as two amine nitrogen and three carbonyl oxygen atoms. They are usually N-coordinated via the negatively charged N atoms [7–14]; however, in some cases, coordination via carbonyl O atoms [15, 16] and C atoms [16, 17] are observed.

Recently, we have started a project on the synthesis and characterization of the metal complexes of 5,5-diethylbarbituric acid (barbH), also known as barbital or veronal. We have prepared a number of new complexes with various co-ligands [18–26]. The barb ligand is present as either a mono- or dianion and displays different coordination

modes such as a monodentate (N), bidentate chelating (N, O), bidentate bridging (N, O), tridentate bridging (N, O, O) and tetradentate bridging (N, N, O, O) ligand. In this paper, we report the syntheses, characterization and crystal structures of two new silver complexes of barb with 2,5-dimethylpyrazine (dmpyz) and piperazine (ppz); namely $[Ag(dmpyz)_2][Ag(barb)_2]$ (**1**) and $\{[Ag(ppz)][Ag(barb)_2]\cdot H_2O\}_n$ (**2**). The thermal decomposition behavior of both complexes was studied and the fluorescent properties of **1** are reported.

2 Experimental

2.1 Materials and Measurements

All commercial reagents were purchased and used as supplied. Elemental analyses for C, H, and N were performed using a Costech elemental analyser. IR spectra were recorded with a Thermo Nicolet 6700 FT-IR spectrophotometer with samples as KBr pellets in the 4,000–400 cm^{-1} range. Thermal analysis data (TGA and DTA) were obtained using a Seiko Exstar 6200 thermal analyzer in a dynamic air atmosphere with a heating rate of 10 °C min^{-1} and a sample size of ca. 10 mg. Excitation and emission spectra of dmpyz and complex **1** were recorded at room temperature in 1×10^{-3} M MeCN solutions with a Varian Cary Eclipse spectrophotometer equipped with a Xe pulse lamp of 75 kW.

2.2 Synthesis of the Silver(I) Complexes

A 10 mL aqueous solution of Na(barb) (5,5-diethylbarbituric acid sodium salt) (0.21 g, 1 mmol) was added to a 10 mL aqueous solution of $AgNO_3$ (0.17 g, 1 mmol) with stirring at room temperature. The solution immediately became milky. The addition of 2,5-dimethylpyrazine (dmpyz) (0.11 mL, 1 mmol) together with a mixture of 2-propanol (PrOH) and acetonitrile (MeCN) (1:1) (10 mL) to the milky suspension resulted in a clear solution. The resulting solution was allowed to stand in darkness at room temperature and colorless crystals of $[Ag(dmpyz)_2][Ag(barb)_2]$ (**1**) were obtained after 3 days. Yield 87%. M.p. 130 °C (decomp). Anal. Calc. for $C_{28}H_{38}N_8O_6Ag_2$ (%): C, 42.1; H, 4.8; N, 14.0. Found: C, 42.3; H, 4.6; N, 14.2%. IR (cm^{-1}): 3175mb, 3077w, 2978m, 2938vw, 2872w, 1712vs, 1679vs, 1634sh, 1601vs, 1491m, 1426vs, 1360vs, 1315vs, 1254s, 1156m, 1054m, 1033m, 976m, 931w, 760m, 686m, 539s, 445s, 412m.

$\{[Ag(ppz)][Ag(barb)_2]\cdot H_2O\}_n$ (**2**) was synthesized in a similar way, replacing dmpyz with ppz. Yield 61%. M.p. 195 °C (decomp). Calc. for $C_{20}H_{34}N_6O_7Ag_2$ (%): C, 35.0; H, 4.5; N, 12.3. Found: C, 35.2; H, 4.4; N, 12.5%. IR (cm^{-1}): 3487mb, 3271m, 3193sb, 3082w, 2966m, 2876w, 1711vs, 1675vs, 1629vs, 1602vs, 1458m, 1419vs, 1368vs, 1317vs, 1257vs, 1279m, 1198w, 1183w, 1165w, 1118m, 1086m, 1031m, 997w, 940m, 881s, 855s, 790w, 763w, 688m, 657w, 635w, 623w, 540s, 478vw, 462w.

2.3 X-ray Crystallography

The intensity data of complexes **1** and **2** were collected using an Enraf–Nonius KappaCCD area detector and STOE IPDS II diffractometers, respectively, with graphite-monochromated Mo K_α radiation ($\lambda = 0.71073$ Å). The structures were solved by direct methods and refined on F^2 with the SHELX-97 program [27]. All non-hydrogen atoms were found from the difference Fourier map and refined anisotropically. All carbon hydrogen atoms were included using a riding model. The water and amine hydrogen atoms in **2** were refined freely. The details of data collection, refinement and crystallographic data are summarized in Table 1.

3 Results and Discussion

3.1 Synthesis and Characterization

Complexes **1** and **2** were obtained in good yields by the reactions with stoichiometric amounts of $AgNO_3$ and Na(barb) in the presence of dmpyz or ppz. In the synthesis, the first white product is insoluble and consists presumably of [Ag(barb)]. However, the product becomes soluble in the PrOH/MeCN solvent mixture. The addition of dmpyz or ppz ligands results in the formation of **1** or **2**. All complexes are non-hygroscopic and stable in air. Complexes **1** and **2** are soluble in water, EtOH and MeCN.

Selected IR data of both complexes are listed in Table 2. The IR spectra of **1** and **2** show characteristic absorption bands of the NH group of barb at 3175 and 3193 cm^{-1}, respectively. The additional bands at 3487 and 3271 cm^{-1} in the spectrum of **2** correspond to the OH vibrations of water and the NH vibrations of the ppz ligand, respectively. The stretching vibrations of the carbonyl groups are observed as three distinct bands in the frequency range 1712–1629 cm^{-1}. Slight changes in the frequency are caused by hydrogen bond interactions. The bands between 1605 and 1250 cm^{-1} are attributed to the C–C, C–N and C–H vibrations of barb, dmpyz and ppz ligands.

3.2 Crystal Structures

The molecular structure of complex **1** is shown in Fig. 1a and the selected bond lengths and angles of **1** are given in Table 3. Complex **1** consists of two ions $[Ag(dmpyz)_2]^+$

Table 1 Crystallographic data and refinement parameters for complexes **1** and **2**

Complex	**1**	**2**
Formula	$C_{28}H_{38}N_8O_6Ag_2$	$C_{20}H_{34}N_6O_7Ag_2$
M	798.40	686.28
T (K)	295 (2)	294 (2)
λ (Å)	0.71073	0.71073
Crystal system	Monoclinic	Orthorhombic
Space group	*C2/c*	*Pnma*
a (Å)	21.5471 (8)	10.5900 (5)
b (Å)	13.4041 (4)	24.6539 (12)
c (Å)	13.3633 (5)	10.1181 (5)
β (°)	125.137 (2)	90
V (Å^3)	3156.28 (19)	2641.7 (2)
Z	4	4
D_{calcd} (g cm^{-3})	1.680	1.726
μ (mm^{-1})	1.290	1.532
θ range (°)	1.91–26.50	2.18–27.50
Index range (h, k, l)	−26/25, −16/16, −16/16	−13/13, −31/32, −13/8
Reflections collected	16824	17629
Data/parameters	3277/204	3100/178
Goodness-of-fit on F^2	1.064	1.029
R_1 [$I > 2\sigma$]	0.0252	0.0257
wR_2 [$I > 2\sigma$]	0.0685	0.0599

Table 2 Selected IR spectral data for **1** and **2**

	1	**2**
ν(OH)	–	3487mb
ν(NH)amine	–	3271m
ν(NH)barb	3175mb	3193sb
ν(CH)	3077w, 2978m, 2872w	3082w, 2966m, 2876w
ν(CO)	1712vs, 1679vs, 1634vs	1711vs, 1675vs, 1629vs

Frequencies in cm^{-1}

b Broad, *w* weak, *vs* very strong, *s* strong, *m* medium, *sh* shoulder

and $[Ag(barb)_2]^-$. In each ion, silver(I) is linearly coordinated by two dmpyz or barb ligands. The linear units are interacted perpendicularly with each other via the Ag···Ag interactions. The distance between two silver centers is 2.896 (1) Å, which is considerably less than the sum of the van der Waals' radii of two silver atoms (3.44 Å), showing a strong interaction between the silver(I) ions, since the upper limit for an Ag–Ag contact in silver(I) complexes is estimated as 3.30 Å [28]. The two barb and two dmpyz ligands are not coplanar. The dihedral angle between the pyrimidine rings of two barb ligands is 79.86 (6)° and the two pyz rings are also oriented with a dihedral angle of 82.51 (7)°. The Ag–N(barb) bond distance in **1** is slightly longer than those of the reported silver(I) complexes containing barb ligands [13, 19, 22, 25, 26], while the Ag–N(dmpyz) bond distance is significantly shorter than those reported for silver(I) pyrazine complexes [29–32].

In addition to the electrostatic interactions between the opposite ions, the $[Ag(barb)_2]^-$ units are doubly bridged by N–H···O bonds involving the barb moieties of the adjacent complexes, which leads to one-dimensional supramolecular chains. As shown in Fig. 1b, these chains are connected into a two-dimensional array, extending along the crystallographic *ac* plane, by weak π(pyz)–π(pyz) stacking interactions with a plane-to-plane distance of 3.778 Å. The two-dimensional layers are further linked into a three-dimensional supramolecular network by C–H···π(pyz) interactions with distances ranging from 3.225 to 3.265 Å.

Complex **2** is a one-dimensional coordination polymer in which the silver(I) ions are linearly bridged by neutral ppz ligands in a zigzag manner to form a cationic $[Ag(ppz)]_n^+$ chain. The $[Ag(barb)_2]^-$ anions (Figs. 2a, b), which contain a silver(I) ion linearly coordinated by two barb ligands, interact with the cationic chain through the Ag···Ag interactions at a distance of 3.183 (1) Å. This distance is considerably shorter than the upper limit of 3.30 Å. Again, the orientation of the $[Ag(barb)_2]^-$ units with respect to the cationic chain is almost perpendicular. In contrast to **1**, the barb rings in $[Ag(barb)_2]^-$ are nearly co-planar with a dihedral angle of 6.74 (5)°. On the other hand, the piperazine ring shows a chair conformation. The Ag–N(barb) bond distance is somewhat shorter than in **1**, while the Ag–N(ppz) bond distances are shorter than found in similar ppz complexes of silver(I) [33, 34].

The structure of complex **2** exhibits an interesting hydrogen bonding scheme (Table 3). The 1D chains running along the *a* axis are bridged by the water molecules via N–H···OW and OW–H···O hydrogen bonds that involve the amine group of ppz and the carbonyl group of barb. This results in a hydrogen-bonded two-dimensional network parallel to the *ac* crystallographic plane (Fig. 2c). These layers are further interconnected by N–H···O hydrogen bonds into a three-dimensional supramolecular network in the solid state.

3.3 Photoluminescence

Complex **1** is luminescent at room temperature, whereas complex **2** is not emissive as expected. This is mainly due to the absence of luminescent chromophores in **2**. The photoluminescence spectra of dmpyz and **1** in MeCN at ambient temperature is depicted in Fig. 3. The electronic spectra of the dmpyz and complex **1** show two absorption

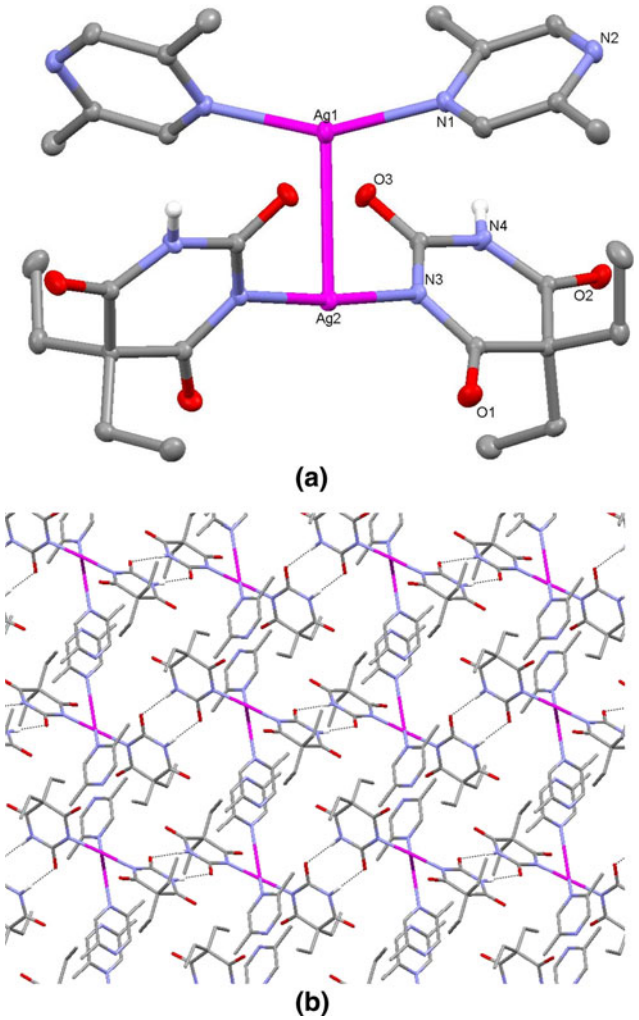

Fig. 1 **a** Molecular structure of **1** with atom labeling. CH hydrogen atoms are omitted for clarity. **b** Packing of molecules of **1** viewed down the *b* axis

maxima at ca. 272 and 307 nm, which are attributed to the π–π^* transitions of the dmpyz ligand. The ligand and complex **1** are not emissive when excited at these absorption wavelengths. However, the dmpyz ligand and complex **1** exhibit single emission bands at ca. 345 nm upon excitation at 330 and 295 nm, respectively (Fig. 3). The transitions may be attributed to the ligand-centered π–π^* transitions at the excited state. Emission between d^{10} metal centers is well known [35]. It has been stated that the Ag–Ag interactions can dramatically alter the emissions of silver(I) complexes [36, 37]. However, metal-centered MLCT or 4d → 5s transitions are not possible due to the lack of appreciable red shift. In the present case, close Ag–Ag contact is observed in the crystal lattice of **1**, and also likely to be present in solution. These argentophilic interactions seem to have a significant influence in the emission intensity of the complex compared to the free ligand.

Table 3 Selected bond lengths (Å), bond angles (°) and hydrogen bonding parameters for **1** and **2**

	1	**2**
Ag1–N1	2.163 (2)	2.111 (2)
Ag2–N3	2.100 (2)	2.158 (3)
Ag2–N4	–	2.160 (3)
Ag1–Ag2	2.896 (1)	3.183 (1)
N1–Ag1–N1^{i}	153.47 (10)	172.00 (10)
N3–Ag2–N3^{i}	174.90 (10)	–
N3–Ag2–N4^{ii}	–	169.79 (10)

Hydrogen bonds

D–H···A	D–H (Å)	H···A (Å)	D···A (Å)	D–H···A (°)
1				
N4–H4···O3^{iii}	0.86	2.08	2.940 (3)	174.0
2				
N2–H2···O2^{iv}	0.85 (3)	2.08 (3)	2.926 (2)	172 (2)
N3–H3···O3^{ii}	0.76 (4)	2.70 (3)	3.290 (3)	135.4 (6)
N4–H4···O1W^{v}	0.80 (4)	2.20 (4)	2.999 (5)	179 (4)
O1W–H1···O3^{vi}	0.83 (4)	2.10 (4)	2.921 (3)	174 (4)

Symmetry operations: (i for **1**) $-x + 1, y, -z + 1/2$; (i for **2**) $x, -y + 1/2, z$; (ii) $x - 1/2, y, -z + 3/2$; (iii) $-x + 1/2, -y + 1/2, -z$; (iv) $-x + 1, -y + 1, -z + 1$; (v) $x + 1/2, y, -z + 3/2$; (vi) $x - 1/2, y, -z + 1/2$

3.4 Thermal Analysis

Thermal stability and decomposition behaviors of both complexes have been studied by DTA and TG in the flowing atmosphere of air. The DTA and TG curves were illustrated in Fig. 4. The decomposition of complex **1** occurs in three distinct stages. The complex is thermally stable up to 133 °C and the first mass loss takes place between 133 and 186 °C with an endothermic DTA peak at 171 °C. The experimental mass loss of 27.0% corresponds to the elimination of two dmpyz ligands (calcd. 27.1%). The decomposition of the barb moiety is observed in the subsequent stages. The second stage in the range 175–252 °C is endothermic with a mass loss 22.0%, while the third stage between 327 and 364 °C is highly exothermic and results in a mass loss of 22.8%. The total mass loss in the second and third stages is 44.8%, which is consistent with the mass of two barb anions (calcd. 45.9%). The decomposition of **1** ends at 364 °C to give metallic silver as the final product.

Complex **2** dehydrates in the temperature range from 92 to 158 °C with a mass loss of 2.5% (calcd. 2.6%). The anhydrous complex is stable to 195 °C and then, shows a continuous mass loss between 195 and 461 °C (Fig. 4). Although it is impossible to resolve the decomposition steps, the DTA peaks 227 and 272 °C are due to removal of ppz; and, the two exothermic peaks at 372 and 409 °C are

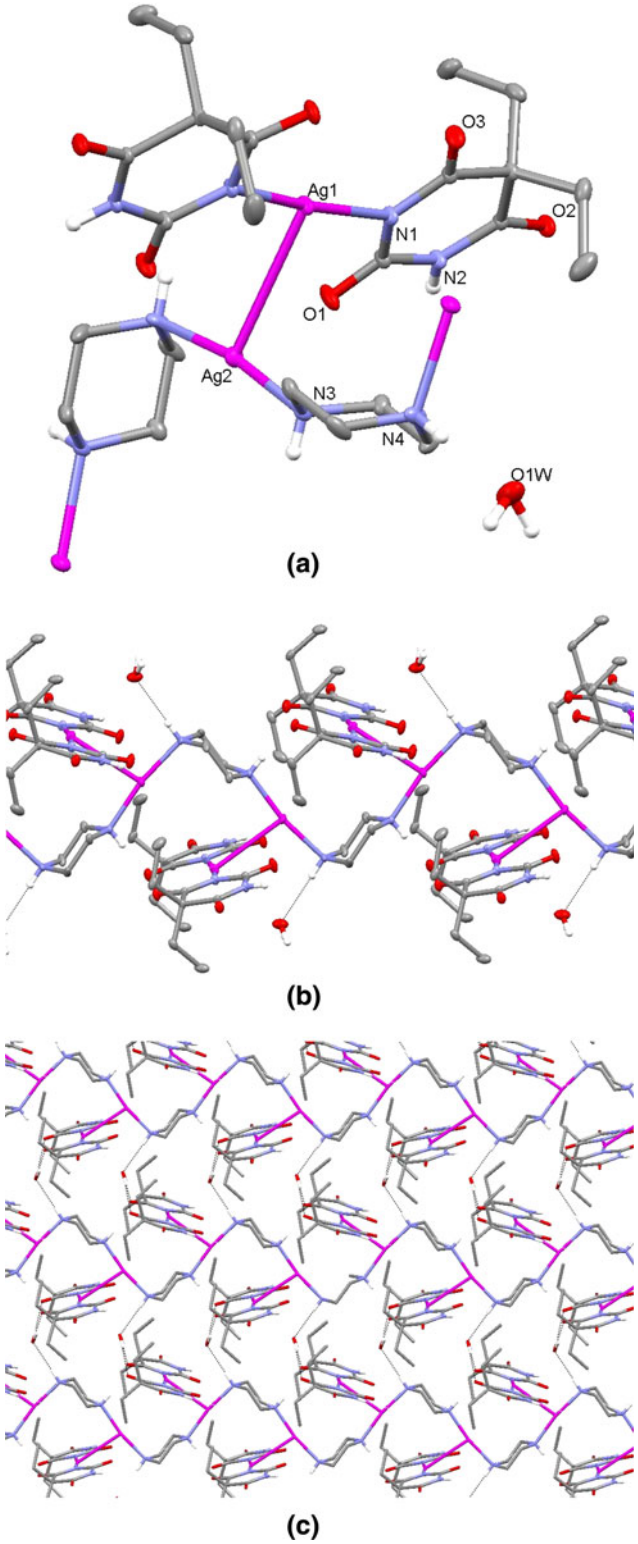

Fig. 2 **a** The building unit of **2** with atom labeling. CH hydrogen atoms are omitted for clarity. **b** A fragment of the one-dimensional chain of **2**. **c** Packing of chains of **2** viewed down the *b* axis

attributed to the decomposition of barb. The total loss of 70.7% (calcd. 68.6%) suggests that the final decomposition product at 461 °C is metallic silver.

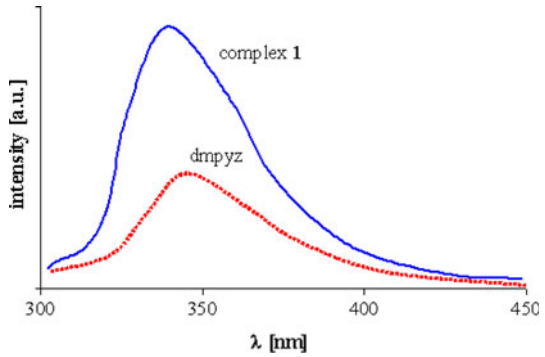

Fig. 3 Emission spectra of dmpyz and complex **1** in MeCN at room temperature

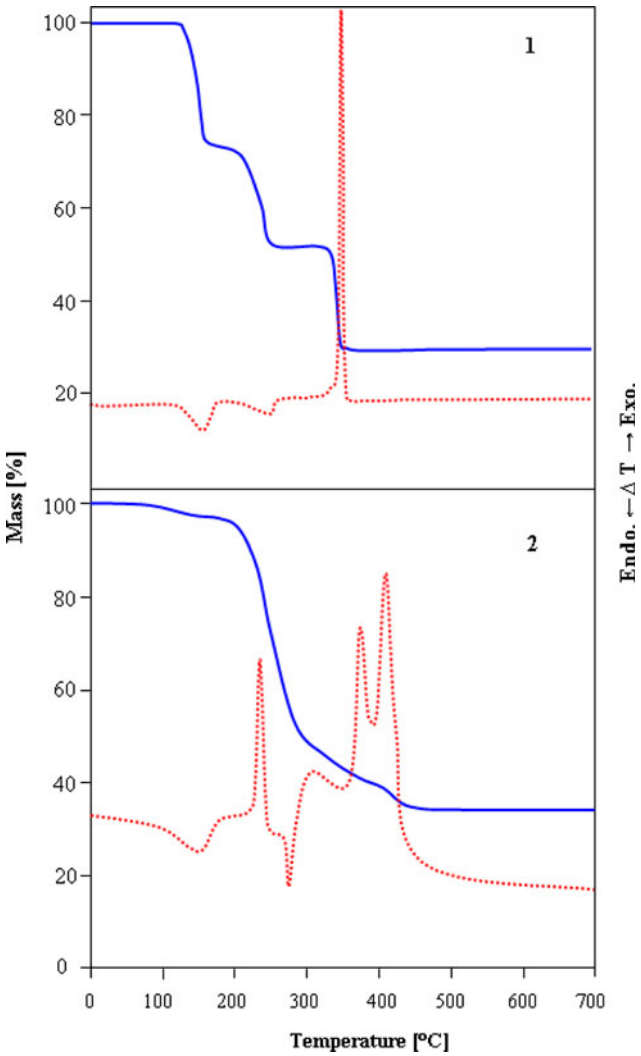

Fig. 4 TG and DTA curves of complexes **1** and **2**

4 Conclusions

Two silver(I) complexes of barb containing the dmpyz and ppz ligands, $[Ag(dmpyz)_2][Ag(barb)_2]$ (**1**) and

$\{[Ag(ppz)][Ag(barb)_2]\cdot H_2O\}_n$ (**2**), have been synthesized and structurally characterized. Both complexes show argentophilic interactions, which play an important role in the construction of complexes in the solid state. Complex **1** exhibits fluorescent emission in solution at room temperature. Thermal decomposition properties of these complexes have been studied.

5 Supplementary Material

Crystallographic data for the structural analysis have been deposited with the Cambridge Crystallographic data center, and CCDC Nos. 760571 and 760572 for compounds **1** and **2**. Copies of this information may be obtained free of charge from the +44(1223)336-033 or Email: deposit@ccdc.cam.ac.uk or www: http://www.ccdc.cam.ac.uk.

Acknowledgments We thank the research fund of Uludag University for the financial support given to the research project (F-2008/56).

References

1. W.J. Doran, Barbituric acid hypnotics, in *Medicinal Chemistry*, vol. 4, ed. by F.F. Blicke, R.H. Cox (Wiley, New York, 1959)
2. I.K. Ho, R.A. Harris, Ann. Rev. Pharmacol. Toxicol. **21**, 83 (1981)
3. J.J.L. Zwicker, Pharm. Weekbl. **68**, 975 (1931)
4. J.C. Umberger, G. Adams, Anal. Chem. **24**, 1309 (1952)
5. L. Levi, C.E. Hubley, Anal. Chem. **28**, 1591 (1956)
6. G.C. Percy, A.L. Rodgers, Spectrosc. Lett. **7**, 431 (1974)
7. B.C. Wang, B.M. Craven, Chem. Commun. 290 (1971)
8. L.R. Nassimbeni, A. Rodgers, Acta Crystallogr. **B30**, 2593 (1974)
9. M.R. Caira, G.V. Fazakerley, P.W. Linder, L.R. Nassimbeni, Acta Crystallogr. **B29**, 2898 (1973)
10. G.V. Fazakerley, P.W. Linder, L.R. Nassimbeni, A.L. Rodgers, Inorg. Chim. Acta **9**, 193 (1974)
11. L. Nassimbeni, A. Rodgers, Acta Crystallogr. **B30**, 1953 (1974)
12. J. Fawcett, W. Henderson, R.D.W. Kemmitt, D.R. Russell, A. Upreti, J. Chem. Soc., Dalton Trans. 1897 (1996)
13. Z.-D. Liua, H.-L. Zhua, Acta Crystallogr. **E60**, m1883 (2004)
14. N. Haque, J.N. Roedel, I.-P. Lorenz, Z. Anorg. Allg. Chem. **635**, 496 (2009)
15. Y. Xiong, C. He, T.C. An, C.H. Cha, X.H. Zhu, Trans. Met. Chem. **28**, 69 (2003)
16. K. Noguchi, H. Yuge, T.K. Miyamato, Acta Crystallogr. **C56**, e40 (2000)
17. K. Noguchi, T. Tamura, H. Yuge, T.K. Miyamato, Acta Crystallogr. **C56**, 171 (2000)
18. F. Yilmaz, V.T. Yilmaz, C. Kazak, Z. Anorg. Allg. Chem. **631**, 1536 (2005)
19. V.T. Yilmaz, F. Yilmaz, H. Karakaya, O. Buyukgungor, W.T.A. Harrison, Polyhedron **25**, 2829 (2006)
20. F. Yilmaz, V.T. Yilmaz, E. Bicer, O. Buyukgungor, Z. Naturforsch. **61b**, 275 (2006)
21. F. Yilmaz, V.T. Yilmaz, E. Bicer, O. Buyukgungor, J. Coord. Chem. **60**, 777 (2007)
22. F. Yilmaz, V.T. Yilmaz, H. Karakaya, O. Buyukgungor, Z. Naturforsch. **63b**, 134 (2008)
23. V.T. Yilmaz, M.S. Aksoy, O. Sahin, Inorg. Chim. Acta **362**, 3703 (2009)
24. M.S. Aksoy, V.T. Yilmaz, O. Buyukgungor, J. Coord. Chem. **62**, 3250 (2009)
25. V.T. Yilmaz, E. Soyer, O. Buyukgungor, J. Organomet. Chem. **694**, 3306 (2009)
26. V.T. Yilmaz, E. Soyer, O. Buyukgungor, Polyhedron **29**, 920 (2010)
27. G.M. Sheldrick, Acta Crystallogr. **A64**, 112 (2008)
28. M. Jansen, Angew. Chem. Int. Ed. Engl. **26**, 1098 (1987)
29. X.-T. Shi, H.-M. Liu, W.-Q. Zhang, J. Mol. Struct. **754**, 37 (2005)
30. S. Hamamci, V.T. Yilmaz, S. Gumus, O. Buyukgungor, Struct. Chem. **19**, 123 (2008)
31. V.T. Yilmaz, E. Senel, E. Guney, C. Kazak, Inorg. Chem. Commun. **11**, 1330 (2008)
32. A.A. Massoud, A. Hefnawy, V. Langer, M.A. Khatab, L. Ohrstrom, Polyhedron **28**, 2794 (2009)
33. S. Hamamci, V.T. Yilmaz, W.T.A. Harrison, J. Mol. Struct. **738**, 191 (2005)
34. V.T. Yilmaz, S. Hamamci, O. Buyukgungor, Polyhedron **27**, 1861 (2008)
35. C. Kutal, Coord. Chem. Rev. **99**, 213 (1990)
36. V.J. Catalano, H.M. Kar, J. Garnas, Angew. Chem. Int. Ed. **38**, 1979 (1999)
37. C. Yue, C. Yan, R. Feng, M. Wu, L. Chen, F. Jiang, M. Hong, Inorg. Chem. **48**, 2873 (2009)